Hindawi
Journal of Food Quality
Volume 2022, Article ID 5565538, 10 pages
https://doi.org/10.1155/2022/5565538

Research Article

Effect of Pretreatment and High Hydrostatic Pressure on Soluble Dietary Fiber in Lotus Root Residues

Yanyang Gu,[1,2] **Liying Niu**,[2] **Jiangfeng Song**,[2] **Chunju Liu**,[2] **Zhongyuan Zhang**,[2] **Chunquan Liu**,[2] **Dajing Li**,[2] **and Lixia Xiao**[1]

[1]*College of Food Science and Engineering, Yangzhou University, Yangzhou 225127, China*
[2]*Institute of Farm Product Processing, Jiangsu Academy of Agricultural Sciences, Nanjing 210014, China*

Correspondence should be addressed to Lixia Xiao; lxxiao@yzu.edu.cn

Received 7 February 2021; Revised 27 November 2021; Accepted 11 January 2022; Published 27 March 2022

Academic Editor: Eduardo Puértolas

High hydrostatic pressure (HHP) can enhance the physicochemical properties of soluble dietary fiber (SDF) from fruit and vegetable residues including hydration properties, emulsibility, and rheological properties, while the pretreatment methods such as solid-water suspension status are ignored all along. Here, three groups of lotus root residue (LRR) for HHP treatment (400 MPa, 15 min) were prepared: the fresh lotus root residue (FLRR), FLRR mixed with water (FLRR + *W*), and dried FLRR suspended in water at the same solid/water level with FLRR + *W* (DLRR + *W*). As a control, non-HHP-treated FLRR was tested. Results showed that FLRR + *W* obtained the highest SDF yield and presented a honeycomb structure which was not observed in other LRR samples. In addition, properties of SDF extract from FLRR + *W* changed most significantly, including not only the enhancement of SDF yield, the improvement of hydration properties, and the reduction of molecular weight but also the increase of thermal and rheological stability. Principal component analysis (PCA) profile illustrated that the difference of LRR-water system contributed 27.6% to the SDF physicochemical changes, and SDF from DLRR + *W* distinguished it from the other samples with mannose, ribose, and glucuronic acid, indicating that the drying procedure also played a role in the HHP treatment focusing on the sugar constitution. Therefore, the solid-water suspension status is a noteworthy issue before HHP treatment aiming at SDF modification.

1. Introduction

Dietary fiber (DF) from fruit and vegetable by-products is well known as a good source of healthy ingredients [1,2]. According to the solution capacity in water, DF can be divided into insoluble dietary fiber (IDF) and soluble dietary fiber (SDF) [3]. Generally, SDF performs superior beneficial properties for human health [4]. Recently, different processing methods have been developed to enhance the SDF distribution as to the improvement of DF function, including chemical [5,6], physical, and biological modifications [7]. Among these methods, high hydrostatic pressure (HHP) is drawing much attention due to its advantages at no chemical involvement, convenience at operation, and high efficiency in DF modification. The effect of HHP on SDF yield enhancement was reported in purple-fleshed potatoes [6], pear pomace [8], and okara by-product from soybean [5]. Moreover, HHP treatment showed a better performance in improving the water-holding and oil-holding capacity, swelling, and cholesterol binding capacity. Yan indicated that, compared with HHP and superfine grinding treatment, the main physicochemical properties of pear pomace of its SDF treated with HHP treatment were significantly improved, including water-holding capacity, oil-holding capacity, expansibility, and cholesterol binding capacity [8].

Before HHP, vacuum packaging was a common method, but the sample status varied. For example, the edible cabbage leaf pieces [9] or grounded fruit peel [10] were directly packed, while the extracted pear peel DF was mixed with distilled water [11]. As it is well known, the fresh tissue from fruit or vegetables always contains not only fibers but also some active enzymes. In the study of the HHP effect on

enzyme activities in Brussels sprouts seedlings, the seedling's water content played an important role under pressure penetration [12]. In another report, the hydrate okara with solid/water (g/mL) 1 : 10 obtained a higher SDF ratio after HHP treatment than the dry sample [5]. Additionally, the starch content (10–70%) in starch-water mixtures would lead to different gelation degrees under HHP treatment [13]. In view of the above-mentioned reports, the different prepared methods may provoke different high-pressure-induced DF modifications.

Lotus root (*Nelumbo nucifera* Gaertn) is an aquatic vegetable in China and is widely consumed due to its unique sensory and nutritional properties [14]. *Lotus* root residue (LRR) is the by-product of the lotus juice processing industry and consists of approximately 30% fresh lotus root weight and is rich in DF [15]. The DF from LRRs is rich in biological activities, including improving immunity [16], regulating lipid metabolism, improving intestinal flora, and preventing diabetes [17]. Meanwhile, this DF has some physiochemical activities, including swelling capacity, water-holding capacity, oil-holding capacity, emulsibility, and rheological properties [15]. Thus, improving the utilization of LRRs and enhancing the output of SDF using HHP technology are attractive prospects. Generally, LRRs keep dried for storage convenience, and HHP is not applicable to food types with low water content [18]. Therefore, the objective of this study was to enhance the SDF yield using HHP treatment as well as to explore the role of water suspension in LRR-SDF extraction. Fresh LRR (FLRR), FLRR mixed with water (FLRR + *W*), and dried LRR (DLRR) mixed with water (DLRR + *W*) were set under HHP treatment. The physicochemical properties, including hydration properties, structural properties, thermal stability, and rheological characteristics of the extracted SDF, were determined and compared.

2. Materials and Methods

2.1. Materials and Reagents. Fresh lotus root (*Nelumbo nucifera* Gaertn) was purchased from the local market (Nanjing, China). The fresh lotus root was washed, sliced, and pressed using a juice squeezer to obtain the wet solid part as the fresh lotus root residues (FLRRs). Some FLRRs were dried at 50°C for 16 h, to obtain the dried LRR (DLRR). The weight of DLRR was 25% (w/w) of the FLRR before drying, so the solid/water ratio of FLRR was about 1 : 3. Then, the FLRR was mixed with distilled water at a ratio of 1 : 5 (W/W) (FLRR + *W*), and the DLRR was mixed with distilled water at a ratio of 1 : 15 (W/W) (DLRR + *W*) as to reach a similar solid/water ratio of FLRR + *W*. After that, the FLRR, FLRR + *W*, and DLRR + *W* were packaged in double nylon/polyester vacuum bags (160 μm thickness with 10 cm × 25 cm size) and vacuum-sealed for HHP treatment, taking the untreated FLRR (FLRR-nH) as the control.

α-Amylase solution (10000 U/mL), protease solution (400 U/mL), and starch glucosidase solution (2000 U/mL) were purchased from Yuanye Bio-Technology Co., Ltd. (Shanghai, China). Monosaccharide standards, including mannose (Man), ribose (Rib), glucuronic acid (GlcA), galacturonic acid (GalA), glucose (Glc), galactose (Gal), xylose (Xyl), and arabinose (Ara), were purchased from Sigma Chemical Co. (St. Louis, MO, USA), and rhamnose (Rha), fucose (Fuc) and dextran standard were purchased from Aladdin Chemical Reagent Co., Ltd. (Shanghai, China). All other chemicals used were analytical grade.

2.2. HHP Treatment. High hydrostatic pressure equipment (600 MPa/3–5 L, Bao Tou Kefa High Pressure Technology Co., Ltd., Inner Mongolia, China) was used to modify the LRRs. Water was used as the transmission fluid in the high-pressure chamber, and its temperature was maintained at 30°C before treatment. Vacuum-packaged FLRR, FLRR + *W*, and DLRR + *W* were dumped into the high-pressure chamber separately, and then, the pressure increased to 400 MPa and maintained for 15 min. At last, the pressure was released in 30 s, and then samples were got out immediately.

2.3. Extraction of SDF, IDF, and TDF from LRRs. The FLRR-nH, FLRR, FLRR + *W,* and DLRR + *W* after HHP treatment were dried at 50°C until the moisture content was lower than 5%. The dried samples (10 mg) were mixed with 400 mL of 0.05 M MES-TRIS buffer solution and magnetically stirred at room temperature for 30 min. Then, the LRRs were enzymatically hydrolyzed with α-amylase, protease, and starch glucosidase according to the AOAC method 991.43 [19].

The enzymatic hydrolysate was centrifuged at 3000*g* for 15 min to obtain the supernatant. Four times the supernatant volume of 60°C 95% ethanol was added to collect the precipitate, which was then washed using 15 mL of 78% ethanol, 15 mL of 95% ethanol, and 15 mL of acetone, successively. After washing, the precipitate was vacuum freeze-dried at −50°C for 48 h and SDF was obtained.

The extraction methods of insoluble dietary fiber and total dietary fiber (TDF) were similar to the above steps. IDF was extracted from the sediment of the enzymatic hydrolysate solution. TDF was calculated as the sum of SDF and IDF.

2.4. Scanning Electron Microscopy (SEM). The LRR samples, before and after HHP treatment, were characterized using an EVO LS10 scanning electron microscope (ZEISS Co., Germany), as well as the four extracted SDF samples. The LRR and SDF samples were dried and adhered to double-sided carbon tape and then coated with a thin gold layer. The magnifications were set at 5000× and 3000×. The images were taken at an accelerating voltage of 10 kV.

2.5. Water-Holding, Oil-Holding, and Swelling Capacities

2.5.1. Water-Holding Capacity. SDF (0.2 g, m_1) was mixed with 10 mL of distilled water uniformly in a container at 25°C for 24 h, and the container was sealed with plastic wrap. The mixture was centrifuged at 3000*g* for 10 min, the amounts of supernatant were removed using a pipette, and the remaining supernatant was gently removed with filter paper.

The residue (m_2) was then weighed. The following formula was used to determine the water-holding capacity (WHC):

$$\mathrm{WHC}\left(\frac{g}{g}\right) = \frac{m_2 - m_1}{m_1}, \quad (1)$$

where m_1 is the original weight of the dried sample and m_2 is the final weight of the wet sample.

2.5.2. Oil-Holding Capacity. The 0.2 g of dried powder of SDF (m_1) was shaken and mixed uniformly with 8 mL of rapeseed oil in the vortex (QL-902, Qilinbeier Co., Ltd., Hai Men, China) for 5 min, and the mixture was stood at 25°C for 24 h. Then, the mixture was centrifuged at 3000 g for 10 min, and the amounts of supernatant were removed. The residue (m_2) was weighed. The following formula was used to determine the oil-holding capacity (OHC):

$$\mathrm{OHC}\left(\frac{g}{g}\right) = \frac{m_2 - m_1}{m_1}, \quad (2)$$

where m_1 is the original weight of the dried sample and m_2 is the final weight of the pellet after removing oil.

2.5.3. Swelling Capacity. The swelling capacity (SWC) of SDF was determined as reported by Chen et al. [15]. A total of 0.2 g of dried powder of SDF (m) and 20 mL of distilled water were mixed in a graduated cylinder, sealed with plastic wrap, and equilibrated for 24 h. The SWC was calculated with the following formula:

$$\mathrm{SWC}\left(\frac{mL}{g}\right) = \frac{v_1 - v_0}{m}, \quad (3)$$

where m is the original weight of the dried sample, v_0 is the volume of the original dried sample, and v_1 is the volume of the pellet after swelling.

2.6. Molecular Weight (Mw) Distribution. The molecular weights of four SDF samples were determined by high-performance gel permeation chromatography (HPGPC) with an Agilent 1200 series apparatus (Agilent Technologies, Santa Clara, CA, USA) equipped with a Shodex Ohpak SB-804 HQ column (8.0 × 300 mm) according to a previous method [20]. The column temperature was maintained at 35°C, and the column was eluted with 0.1 M NaCl solution at a flow rate of 0.5 mL/min. Standard D-series dextrans with different molecular weights (D-2, D-3, D-4, D-5, D-6, D-7, and D-8) were used to obtain the calibration curve.

2.7. Monosaccharide Composition. The monosaccharide composition of four SDF samples was determined according to a previously reported method [20] with slight modifications. One hundred microliters of SDF solution (5 mg/mL) was absorbed into a 2.5 mL stopper tube and hydrolyzed with 100 μL of 4 M trifluoroacetic acid (TFA) at 120°C for 2 h. After the hydrolysate was cooled, methanol was added and evaporated to dryness at 50°C three times. Then, 100 μL of deionized water was added to dissolve the residue for the derivatization reaction.

The solution was mixed with 100 μL of 0.6 M NaOH, and then 100 μL of the mixed solution was added to 100 μL of 0.5 M 3-methyl-1-phenyl-2-pyrazoline-5-one (PMP) methanol solution and reacted at 70°C for 100 min. After being cooled to room temperature, 50 μL of 0.3 M HCl was added to neutralize the solution. The reaction mixture was evaporated to dryness at 50°C and dissolved in 1.0 mL of distilled water and 1.0 mL of chloroform, and the excess PMP was then leached with chloroform three times.

The aqueous solution was filtered through a 0.45 μm membrane and determined using an Agilent 1100 HPLC system equipped with a photodiode array detector. The chromatographic conditions were as follows: an Eclipse Plus C18 column (4.6 × 250 mm, 5 μm, Agilent), column temperature 30°C, the mobile phase consisting of phosphate-buffered saline (PBS, 0.1 M, pH 6.7) and acetonitrile (83 : 17, V/V), flow rate 1.0 mL/min, and detector wavelength 245 nm. The injection volume was 20 μL. PMP labeling and HPLC analysis of monosaccharide standards were carried out using the same method.

2.8. Thermal Properties. The thermal properties of SDF samples were analyzed using differential scanning calorimetry (DSC 8000, PerkinElmer Co., USA). The DSC equipment was calibrated using the empty aluminum pan as a reference. Then, 2.0–5.0 mg of each SDF sample was sealed into an aluminum pan and was heated from 30°C to 240°C at a heating rate of 10°C/min under nitrogen. All runs were performed in triplicate. The onset temperature (To), conclusion temperature (Tc), peak temperature (Tp), and enthalpy (ΔH) values were computed with corresponding software.

2.9. Static Rheological Measurements. The rheological measurements of SDF samples were determined at 25°C on a HAAKE MARS 60 rheometer (ThermoFisher Scientific, Germany), which was performed using a cone plate with an angle of 2° (60 mm diameter, 50 μm plate spacing). A 20 mg/mL SDF solution was continuously stirred until completely dissolved and was then equilibrated statically at 25°C for 12 h. The shear stress and apparent viscosity were recorded by a function of shear rate ranging from 0.1 to 100 s^{-1} acquired in a logarithmic ramp. Data acquisition and recording were completed using HAAKE RheoWin software. A power law model was used to describe the rheological properties of the fluids:

$$\text{Power} - \text{law model: } \tau = K\dot{\gamma}^n. \quad (4)$$

Here, τ is the shear stress (Pa), $\dot{\gamma}$ is the shear rate (s^{-1}), K is the consistency index (Pa·s^n), and n is the power law index.

2.10. Statistical Analysis. Each experiment was performed in triplicate. The data from the experiments are expressed as the mean ± standard deviation. Analysis of variance (ANOVA) with Duncan's test of the differences between groups was

carried out using Statistical Package for the Social Sciences (SPSS, version 22.0, SPSS Inc., Chicago, Illinois, USA). $p < 0.05$ indicated a statistically significant difference. PCA was used to determine the relationships among the extraction rate, hydration properties, molecular weight, thermal stability, rheological property, and monosaccharide content using JMP 10 (SAS Institute Inc., NC, USA).

3. Results and Discussion

3.1. Extraction Rate of the DF Fraction from LRRs. Table 1 shows the SDF, IDF, and TDF constituents of LRR samples. The SDF yields all increased significantly after HHP treatment. The extraction yields of SDF from high hydrostatic pressure treated FLRR, FLRR + *W*, and DLRR + *W* were 10.15%, 10.50%, and 9.85%, respectively. Compared with the sample without HHP-treated (FLRR-nH-SDF, 9.2%), HHP enhanced the SDF yield significantly ($p < 0.05$) in all kinds of sample preparations. Therefore, HHP was beneficial for more SDF released from the cell wall, leading to an increased extraction yield. This phenomenon was consistent with the former reports [6,21]. Meanwhile, there were no significant differences among the TDF contents of FLRR-nH, FLRR, and DLRR + *W*, suggesting the SDF enhancement was due to the IDF, such as cellulose and hemicelluloses, degraded under HHP.

In this study, the SDF extraction rates of LRRs after HHP treatment showed a significant difference ($p < 0.05$) depending on different solid/water statuses although they had experienced the same HHP treatment. The FLRR + *W* obtained the highest extraction rate of SDF, while DLRR + *W* was the lowest. The SDF content of FLRR + *W* was higher than that of FLRR, indicating that the role of water in the suspension system of FLRRs could not be neglected. Typically, water was used as the pressure transfer medium at HHP treatment, which set samples under uniform stress to achieve a better penetration [18]. Additionally, FLRR + *W* showed higher SDF content than DLRR + *W*, although it was suspended with a similar solid/water ratio. In reports, the drying procedure may lead to enzyme inactivation [22] and physical structure changes [23], which possibly hamper the DF modification.

3.2. SEM Observation. The SEM micrographs of LRR samples are shown in Figure 1 under a magnification of 5000×. From the images, the surface of the FLRR-nH structure was relatively smooth with no large wrinkles. However, irregular wrinkles appeared on the surface of three HHP-treated LRR samples. Compared with the FLRR, FLRR + *W* exhibited a loose structure with honeycombed protuberance and depression, while DLRR + *W* demonstrated flaky fragmentation. According to the SEM micrographs of SDF samples, the samples that experienced HHP treatment shaped ridges and valleys with more particles adhered, contrasting that of FLRR-nH-SDF which was flat and smooth. These results were consistent with former studies that reported that HHP could have loose and rough plant tissue [6,24]. Among the HHP-treated samples, no matter LRR or SDF, the deformation of FLRR + *W* was most prominent, suggesting its distinctive physicochemical properties.

3.3. Analysis of Water-Holding, Oil-Holding, and Swelling Capacities. The water-holding, oil-holding, and swelling capacities of SDF from LRRs subjected to different treatments are shown in Table 2. The WHC, OHC, and SWC values were increased significantly after HHP treatment. The result might be that HHP changed the structure of SDF; i.e., looser and rougher surfaces increased the volume of water and oil absorption [25, 26].

In addition, results showed that FLRR + W-SDF had the maximum hydration values which were 2.13–2.72 times higher than that of FLRR-nH-SDF, as well as 1.42–1.93 times higher than those values of FLRR-SDF and DLRR + W-SDF. The distinctive improved hydration properties of FLRR + W-SDF are probably associated with its prominent structure change observed in Figure 1. Since no significant difference ($p > 0.05$) was observed between FLRR-SDF and DLRR + W-SDF, the assistance of water dispersion for HHP penetration in dried LRR was not manifested, which might be due to differences in porosity, the higher SDF content, and porous structure corresponding to the improvement of WHC [27].

3.4. Molecular Weight and Monosaccharide Composition Analysis. The Mw values of SDF samples from FLRR-nH, FLRR, FLRR + *W*, and DLRR + *W* were determined to be 1268 kDa, 1167 kDa, 1127 kDa, and 1137 kDa, respectively (Table 3). HHP reduced the Mw value, in a percentage range of 7.96%–11.12%. This phenomenon could be explained by the partial degradation of SDF caused by HHP treatment, including the disruption of intramolecular hydrogen bonds and the releasement of low Mw soluble molecules [28–31].

The Fourier-transform infrared spectroscopy (FT-IR) spectra of SDF from LRRs exhibited a typical absorption property of polysaccharides (Supplemental Figure S1). The SDF samples from LRRs which were composed of eight monosaccharides are quantified and listed in Table 3, namely, Man, Rib, GlcA, GalA, Glc, Gal, Ara, and Fuc. Glc was the main constituent of all the four samples with a molar percentage from 43.01 mol% to 47.46 mol%, followed by Gal (14.01 mol%-18.42 mol%), which was similar to previous research studies about lotus root polysaccharides [32, 33]. Glc is the main constitute suggesting the presence of glucan. Considering that amylose glucosidase can efficiently hydrolyze a portion of starch of LRR to glucose [15] and starch could precipitate with fiber, the high percentage of glucose was probably in part to starch. Additionally, Fuc was the second abundant monosaccharide only detected in the SDF sample without HHP pretreatment. The reason for this difference was probably coming from the bond disrupt effect due to HHP, which lead to the loss of Fuc during extraction [34]. On the other hand, the sum of the four monomeric sugars including GlcA, Gal, GalA, and Ara, which are typical pectin compositions, accounted for 32.16 mol%-50.03 mol% of the total monosaccharide, indicating that pectin might be one of the main components of LRR-SDF [35]. For the

Table 1: Extraction rates of DF fraction from LRRs.

Extraction rate	SDF (%)	IDF (%)	TDF (%)
FLRR-nH	9.20 ± 0.08^{c}	26.75 ± 0.04^{a}	35.95 ± 0.04^{a}
FLRR	10.15 ± 0.20^{ab}	25.95 ± 0.20^{b}	36.10 ± 0.41^{a}
FLRR + *W*	10.50 ± 0.24^{a}	24.65 ± 0.04^{c}	35.15 ± 0.29^{b}
DLRR + *W*	9.85 ± 0.04^{b}	26.60 ± 0.16^{a}	36.45 ± 0.12^{a}

Values are means ± SD of triplicates. Values in the same column with different superscripts are significantly different ($p < 0.05$).

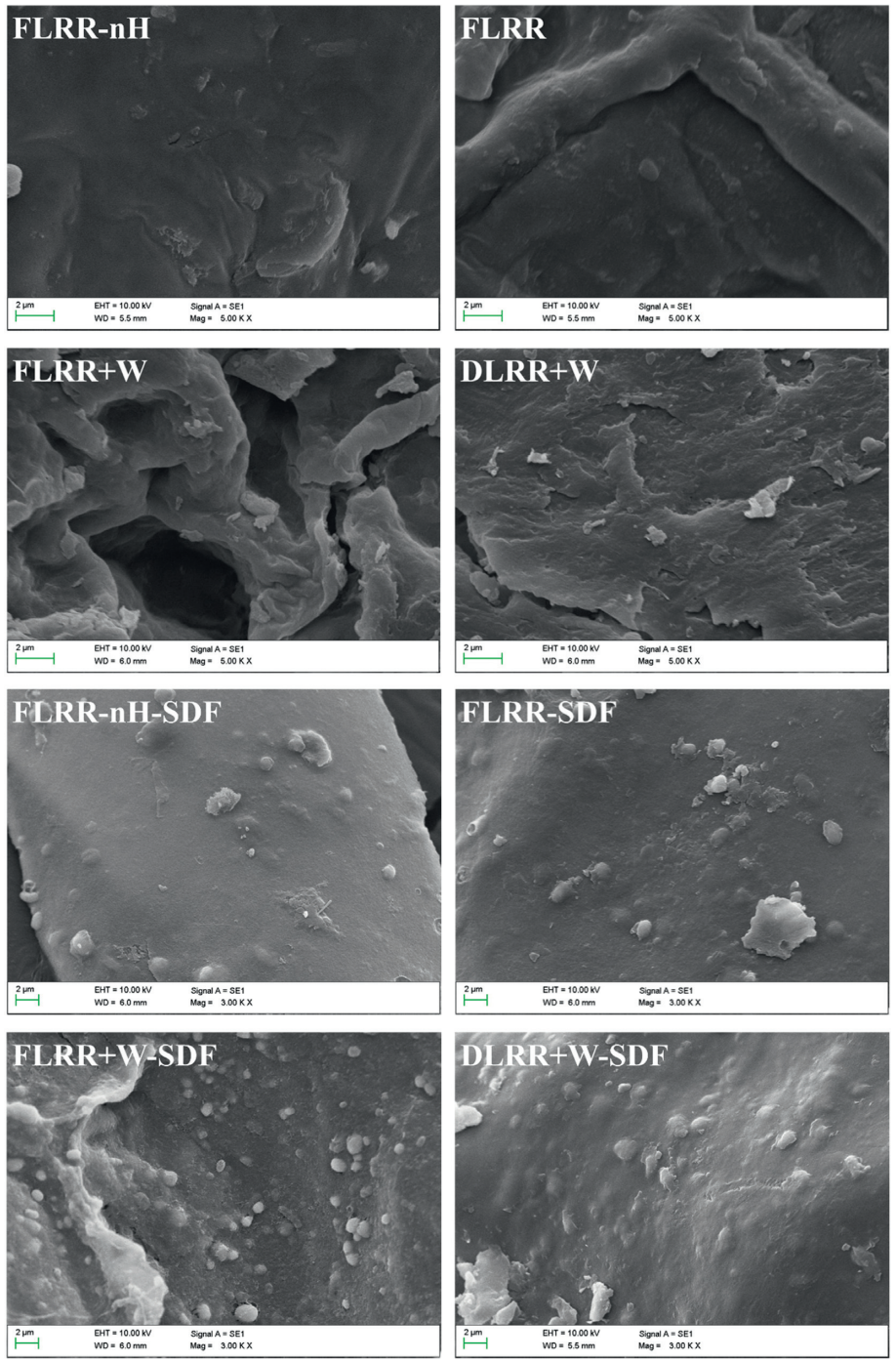

Figure 1: Scanning electron microscopy microstructure images of the LRR at 5000x magnification (FLRR-nH, FLRR, FLRR + *W*, and DLRR + *W*) and SDF from LRRs at 3000x magnification (FLRR-nH-SDF, FLRR-SDF, FLRR + W-SDF, and DLRR + W-SDF).

Table 2: Water-holding, oil-holding, and swelling capacities of FLRR-nH-SDF, FLRR-SDF, FLRR + W-SDF, and DLRR + W-SDF samples from LRRs.

Sample	WHC (g/g)	OHC (g/g)	SWC (mL/g)
FLRR-nH-SDF	2.52 ± 0.09^{c}	1.54 ± 0.08^{c}	2.03 ± 0.10^{c}
FLRR-SDF	2.80 ± 0.16^{bc}	2.55 ± 0.12^{b}	3.12 ± 0.05^{b}
FLRR + W-SDF	5.39 ± 0.17^{a}	4.19 ± 0.28^{a}	4.94 ± 0.15^{a}
DLRR + W-SDF	3.07 ± 0.03^{b}	2.95 ± 0.09^{b}	3.29 ± 0.13^{b}

Values are means ± SD of triplicates. Values in the same column with different superscripts are significantly different ($p < 0.05$).

Table 3: Molecular weights and monosaccharide compositions of FLRR-nH-SDF, FLRR-SDF, FLRR + W-SDF, and DLRR + W-SDF samples from LRRs.

	FLRR-nH-SDF	FLRR-SDF	FLRR + W-SDF	DLRR + W-SDF
Mw (kDa)	1268 ± 3.674^{a}	1167 ± 5.552^{b}	1127 ± 2.449^{d}	1137 ± 4.572^{c}
Monosaccharide compositions (mol%)				
Man	4.12 ± 0.09^{b}	3.85 ± 0.02^{c}	3.58 ± 0.16^{d}	5.16 ± 0.03^{a}
Rib	3.09 ± 0.12^{b}	2.89 ± 0.10^{c}	2.67 ± 0.06^{d}	3.90 ± 0.02^{a}
GlcA	9.31 ± 0.07^{bc}	9.36 ± 0.29^{b}	8.95 ± 0.14^{c}	12.56 ± 0.06^{a}
GalA	3.11 ± 0.12^{c}	5.65 ± 0.10^{b}	5.87 ± 0.21^{b}	6.76 ± 0.03^{a}
Glc	43.01 ± 0.19^{c}	43.22 ± 0.33^{c}	46.66 ± 0.20^{b}	47.46 ± 0.07^{a}
Gal	14.01 ± 0.10^{d}	16.65 ± 0.20^{c}	18.42 ± 0.16^{a}	17.72 ± 0.16^{b}
Ara	5.73 ± 0.02^{d}	18.37 ± 0.04^{a}	13.85 ± 0.09^{b}	6.44 ± 0.07^{c}
Fuc	17.63 ± 0.20^{a}	nd	nd	nd

Values are means ± SD of triplicates. Values in the same row with different superscripts are significantly different ($p < 0.05$). nd: not detected.

HHP-treated SDF samples, FLRR-SDF and FLRR + W-SDF exhibit an evidently high percentage of Ara and it can conclude the presence of arabinogalactan-proteins with Fuc residues adjacent Ara residues in LRRs [36]. Moreover, the less percentage of Ara in DLRR + W-SDF might indicate that the drying procedure reduced the Ara residue in the polysaccharide.

3.5. Thermal Analysis. As indicated in Figure 2, the DSC curves in the range of 30–240°C of four SDF samples each exhibit an exothermic peak. The To, Tc, Tp, and △H values are listed in Table 4. In this analysis, dried SDF samples were determined directly, so the exothermic temperature values between 176.20°C and 182.82°C should be due to the decomposition of carbohydrates [37].

Compared with the SDF sample from FLRR-nH, the HHP procedure increased the stability temperature and decreased the enthalpy change value, which certified that the HHP treatment could improve the thermal stability [38] and reduce the phase transformation energy of SDF. Besides, only the values of FLRR + W-SDF showed a significant difference with FLRR-nH-SDF. As well known, HHP can break the intermolecular hydrogen bonds and promotes the formation of intermolecular hydrogen bonds with water [39]; these changes were possibly correlated with the more intermolecular hydrogen bonds formed in FLRR + W-SDF. This conclusion strongly agreed with the previous results obtained from soybean residue SDF [40].

3.6. Rheological Properties. The variation of shear stress on the shear rate at the same concentration of SDF solution is shown in Figure 3. The shear stress of all the samples

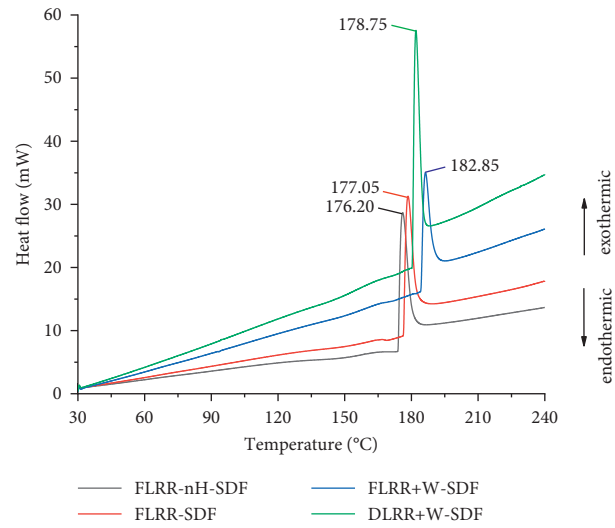

Figure 2: DSC curves of FLRR-nH-SDF, FLRR-SDF, FLRR + W-SDF, and DLRR + W-SDF from LRRs.

increased with the increase of the shear rate. the curve of the FLRR-nH-SDF was prominent compared with the other three samples, and the curves of SDF extracted from FLRR + *W*, FLRR, and DLRR are arranged in a descending sequence. According to the SEM graph, the surface of FLRR-nH-SDF was flat, which may be more stable with a high shear rate than the other three modified SDF.

The power law model fits the rheological models well ($R^2 > 0.97$), and the parameters of the models are listed in Table 5. The SDF suspension fluids were shear-thinning for $n < 1$ [41], which means that the viscosity will decrease with the increase in the shearing. However, FLRR + W-SDF

Table 4: Thermodynamic properties of FLRR-nH-SDF, FLRR-SDF, FLRR + W-SDF, and DLRR + W-SDF samples from LRRs.

Sample	To (°C)	Tc (°C)	Tp (°C)	△H (J/g)
FLRR-nH-SDF	174.14 ± 0.33^{b}	181.18 ± 0.93^{b}	176.20 ± 0.50^{b}	280.97 ± 1.13^{a}
FLRR-SDF	175.37 ± 0.86^{b}	180.81 ± 1.21^{b}	177.05 ± 1.01^{b}	243.19 ± 1.58^{ab}
FLRR + W-SDF	181.12 ± 1.92^{a}	186.68 ± 2.28^{a}	182.85 ± 2.15^{a}	203.31 ± 2.36^{b}
DLRR + W-SDF	176.89 ± 2.03^{ab}	183.63 ± 1.19^{ab}	178.75 ± 2.13^{ab}	248.83 ± 2.33^{a}

Values are means ± SD of triplicates. Values in the same column with different superscripts are significantly different ($p < 0.05$).

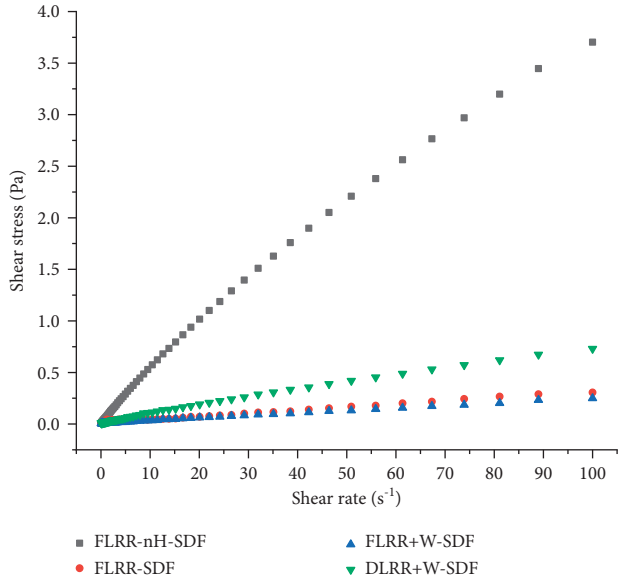

Figure 3: Shear stress versus shear rate profiles of FLRR-nH-SDF, FLRR-SDF, FLRR + W-SDF, and DLRR + W-SDF from LRRs.

Table 5: Rheological properties of FLRR-nH-SDF, FLRR-SDF, FLRR + W-SDF, and DLRR + W-SDF samples from LRRs.

Sample	K (Pa·s^n)	n	R^2
FLRR-nH-SDF	0.0833 ± 0.0012^{a}	0.8302 ± 0.0033^{b}	0.9996
FLRR-SDF	0.0071 ± 0.0007^{c}	0.8163 ± 0.0236^{c}	0.9734
FLRR + W-SDF	0.0048 ± 0.0002^{d}	0.8532 ± 0.0116^{a}	0.9944
DLRR + W-SDF	0.0159 ± 0.0002^{b}	0.8329 ± 0.0033^{b}	0.9995

Values are means ± SD of triplicates. Values in the same column with different superscripts are significantly different ($p < 0.05$).

showed the highest n value than the other three samples, suggesting its pseudoplasticity degree was weaker. The consistency index (K) provides a measure of the viscosity of materials at very low shear rates, and the higher the consistency index is, the higher the viscosity of the sample is [42]. Compared with FLRR-nH-SDF, the SDF extracted from HHP-treated LRRs showed significantly lower K values, which accounted for approximately one-tenth to one-fifth of the K value of FLRR-nH-SDF. It illustrated that HHP-treated SDF showed better properties for food stirring when a smaller influence of stirring speed was needed. According to the study of Li et al. [43], the viscosity of SDF correlated with the molecular chain arrangement; the lower K values of the HHP-treated SDF may be due to their lower molar mass sequences (Table 3), which gives the molecules higher mobility and greater possibility of forming junctions with neighboring chains. Furthermore, there is dietary fiber's rheological behavior in the solution and gel states, which are controlled by their molecular features, such as their Mw [44].

3.7. Correlation Analysis of SDF Physiochemical Attributes. Pairwise correlation analysis was performed using the Pearson method, and the clustered correlation colormap is shown in Figure 4(a). The extraction rate, WHC, OHC, SWC, Tp, Ara, GalA, Gal, and Glc showed positive correlations, and they clustered and formed a red square in Figure 4(a) as group I. Mw, K, and Fuc showed negative correlations, displayed in blue color with parameters of group I, and formed group II. The last three parameters, Man, Rib, and GlcA, showed significant positive correlations with each other ($r > 0.9$, $p < 0.01$), and weak correlations with the parameters in group I and group II and were thus marked as group III.

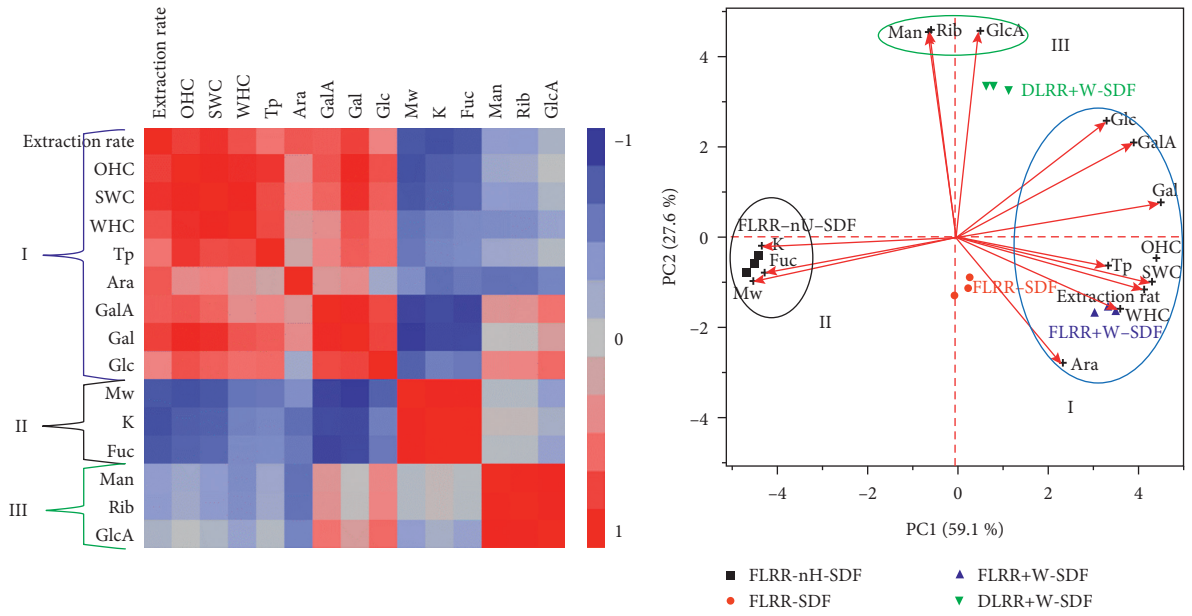

(a) (b)

Figure 4: Heat map of the cluster correlation (a) and PCA profile (b) of the indicator data of FLRR-nH-SDF, FLRR-SDF, FLRR + W-SDF, and DLRR + W-SDF from LRRs.

A previous study indicated that the viscosity was positively associated with the Mw [45], and results in this study are consistent with it. The positive correlations among the extraction rate, hydration property, thermal stability, and monosaccharide in group I imply the molecule changes, and these physical properties were synchronous to HHP treatment, which might reflect the characters of the main polysaccharide composition of SDF, such as pectin or glucan. Additionally, the extremely positive correlation of Mw, *K*, and Fuc in group II, indicating that the change of Mw was the main factor, and affected the viscosity. Besides, Man, Rib, and GlcA were not the main constituent of SDF, inferring that they were originated from the same molecule.

In this study, principal component analysis (PCA) was performed to obtain an overview of the relationship among all digital parameters. The first two components explained 86.7% of the total variation, and the PCA profile is shown as a biplot (Figure 4(b)). The FLRR-nH-SDF was close to group II and located on the left part with negative PC1 scores, distinguishing it from the other three samples. Moreover, FLRR-nH-SDF showed the farthest distance to group I on PC1, opposing FLRR + W-SDF. Considering that FLRR-SDF and DLRR + W-SDF were located between FLRR-nH-SDF and FLRR + W-SDF, it seemed that PC1 mainly showed the reaction of HHP treatment on modifying SDF from LRRs. In addition, the DLRR + W-SDF was located on the upper part with a positive PC2 score, while FLRR-nH-SDF, FLRR-SDF, and FLRR + W-SDF samples obtained a negative PC2 score. In view of the DLRR + W-SDF being the only one that had endured drying before HHP treatment and was close to group III, it seemed that PC2 classified the samples with or without drying procedures via the differences in Man, Rib, and GlcA in group III.

4. Conclusion

In this study, HHP treatment significantly improved the LRR physiochemical properties. However, the preparation method before treatment could not be neglected. LRRs in different water suspension statuses responded differently to HHP treatment. FLRR + *W* presented the most prominent response than FLRR and DLRR + *W*. Moreover, FLRR + W-SDF was superior to FLRR-SDF at the hydration, thermal, and rheological characters. On the other side, the DLRR + W-SDF showed inferior physicochemical properties to FLRR + W-SDF, though the LRRs where they were extracted from were at a similar solid/water ratio. Furthermore, from the PCA profile, HHP treatment was the major effect for physicochemical changes when compared with FLRR-nH-SDF, and DLRR + W-SDF separated with the other three samples suggesting drying arose a special effect on DF modification. Ultimately, the solid-water suspension status is deserved to pay close attention to for DF modification, and drying is not recommended before using HHP treatment.

Data Availability

All data and analyses are reported in the tables and figures.

Conflicts of Interest

The authors declare that they have no conflicts of interest.

Authors' Contributions

Yanyang Gu did parameter determination and wrote the original draft of the manuscript. Liying Niu contributed to the supervision, writing the original draft, and

reviewing and editing the manuscript. Liying Niu and Yanyang Gu contributed equally to this paper. Jiangfeng Song did the HHP equipment operation and draft revision. Chunju Liu, Zhongyuan Zhang, Dajing Li, and Chunquan Liu contributed to the interpretation of data and discussion of the related results. Lixia Xiao contributed to the design of the work and the improvement of the analysis.

Acknowledgments

The authors are grateful for the financial support of the Primary Research and Development Plan of Jiangsu Province (no. BE2019335).

Supplementary Materials

Figure S1: infrared spectroscopy readouts of FLRR-nH-SDF, FLRR-SDF, FLRR + W-SDF, and DLRR + W-SDF samples from LRRs. (*Supplementary Materials*)

References

[1] N. O'Shea, E. K. Arendt, and E. Gallagher, "Dietary fibre and phytochemical characteristics of fruit and vegetable by-products and their recent applications as novel ingredients in food products," *Innovative Food Science & Emerging Technologies*, vol. 16, pp. 1–10, 2012.

[2] P. C. K. Cheung, "Mini-review on edible mushrooms as source of dietary fiber: preparation and health benefits," *Food science and human wellness*, vol. 2, no. 3-4, pp. 162–166, 2013.

[3] F.-J. Dai and C.-F. Chau, "Classification and regulatory perspectives of dietary fiber," *Journal of Food and Drug Analysis*, vol. 25, no. 1, pp. 37–42, 2017.

[4] H. B. Sowbhagya, P. F. Suma, S. Mahadevamma, and R. N. Tharanathan, "Spent residue from cumin - a potential source of dietary fiber," *Food Chemistry*, vol. 104, no. 3, pp. 1220–1225, 2007.

[5] I. Mateos-Aparicio, C. Mateos-Peinado, and P. Rupérez, "High hydrostatic pressure improves the functionality of dietary fibre in okara by-product from soybean," *Innovative Food Science & Emerging Technologies*, vol. 11, no. 3, pp. 445–450, 2010.

[6] F. Xie, M. Li, X. Lan et al., "Modification of dietary fibers from purple-fleshed potatoes (Heimeiren) with high hydrostatic pressure and high pressure homogenization processing: a comparative study," *Innovative Food Science & Emerging Technologies*, vol. 42, pp. 157–164, 2017.

[7] C. Wang, R. Song, S. Wei et al., "Modification of insoluble dietary fiber from ginger residue through enzymatic treatments to improve its bioactive properties," *Lebensmittel-Wissenschaft & Technologie*, vol. 125, p. 109220, 2020.

[8] L. Yan, T. Li, C. Liu, and L. Zheng, "Effects of high hydrostatic pressure and superfine grinding treatment on physico-chemical/functional properties of pear pomace and chemical composition of its soluble dietary fibre," *Lebensmittel-Wissenschaft & Technologie*, vol. 107, pp. 171–177, 2019.

[9] M. Wennberg and M. Nyman, "On the possibility of using high pressure treatment to modify physico-chemical properties of dietary fibre in white cabbage (*Brassica oleracea* var. capitata)," *Innovative Food Science & Emerging Technologies*, vol. 5, no. 2, pp. 171–177, 2004.

[10] V. Tejada-Ortigoza, L. E. Garcia-Amezquita, V. Serment-Moreno, J. A. Torres, and J. Welti-Chanes, "Moisture sorption isotherms of high pressure treated fruit peels used as dietary fiber sources," *Innovative Food Science & Emerging Technologies*, vol. 43, pp. 45–53, 2017.

[11] G. Yu, J. Bei, J. Zhao, Q. Li, and C. Cheng, "Modification of carrot (Daucus carota Linn. var. Sativa Hoffm.) pomace insoluble dietary fiber with complex enzyme method, ultrafine comminution, and high hydrostatic pressure," *Food Chemistry*, vol. 257, pp. 333–340, 2018.

[12] J. Wang, F. J. Barba, J. C. Sørensen et al., "The role of water in the impact of high pressure on the myrosinase activity and glucosinolate content in seedlings from Brussels sprouts," *Innovative Food Science & Emerging Technologies*, vol. 58, p. 102208, 2019.

[13] H. E. Oh, D. N. Pinder, Y. Hemar, S. G. Anema, and M. Wong, "Effect of high-pressure treatment on various starch-in-water suspensions," *Food Hydrocolloids*, vol. 22, no. 1, pp. 150–155, 2008.

[14] P. Dong, M. Kong, J. Yao et al., "The effect of high hydrostatic pressure on the microbiological quality and physicochemical properties of lotus root during refrigerated storage," *Innovative Food Science & Emerging Technologies*, vol. 19, pp. 79–84, 2013.

[15] H. Chen, C. Zhao, J. Li, S. Hussain, S. Yan, and Q. Wang, "Effects of extrusion on structural and physicochemical properties of soluble dietary fiber from nodes of lotus root," *Lebensmittel-Wissenschaft & Technologie*, vol. 93, pp. 204–211, 2018.

[16] W. Hu, Y. Jiang, Q. Xue et al., "Structural characterisation and immunomodulatory activity of a polysaccharide isolated from lotus (*Nelumbo nucifera* Gaertn.) root residues," *Journal of Functional Foods*, vol. 60, p. 103457, 2019.

[17] Z. Zheng, S. Zhong, and Q. Huang, "Research progress of Lotus root dietary fiber," *The Food Industry*, vol. 42, no. 6, pp. 397–401, 2021.

[18] H.-W. Huang, S.-J. Wu, J.-K. Lu, Y.-T. Shyu, and C.-Y. Wang, "Current status and future trends of high-pressure processing in food industry," *Food Control*, vol. 72, pp. 1–8, 2017.

[19] Aoac, "AOAC official method 991.43 total, soluble, and insoluble dietary fibre in foods," 1998.

[20] Q. Yuan, Y. Xie, W. Wang et al., "Extraction optimization, characterization and antioxidant activity in vitro of polysaccharides from mulberry (*Morus alba* L.) leaves," *Carbohydrate Polymers*, vol. 128, pp. 52–62, 2015.

[21] A. Kokorevics and J. Gravitis, "Cellulose depolymerization to glucose and other water soluble polysaccharides by shear deformation and high pressure treatment," *Glycoconjugate Journal*, vol. 14, no. 5, pp. 669–676, 1997.

[22] W. Mo, K. Ke, X. Shen, and B. Li, "The influence of "thermal drying pretreatment" on enzymatic hydrolysis of cellulose and xylan in poplar fibers with high lignin content," *Carbohydrate Polymers*, vol. 228, p. 115400, 2020.

[23] A. Twarogowska, C. Van Poucke, and B. Van Droogenbroeck, "Chemical composition and functional properties of dietary fibre root powders," *Food Chemistry*, vol. 332, p. 127444, 2020.

[24] J.-K. Yan, L.-X. Wu, W.-D. Cai, G.-S. Xiao, Y. Duan, and H. Zhang, "Subcritical water extraction-based methods affect the physicochemical and functional properties of soluble dietary fibers from wheat bran," *Food Chemistry*, vol. 298, p. 124987, 2019.

[25] N. Baenas, V. Nuñez-Gómez, I. Navarro-González, L. Sánchez-Martínez, J. García-Alonso, and M. J. González-Barrio, "Raspberry dietary fibre: chemical properties,

functional evaluation and prebiotic in vitro effect," *Lebensmittel-Wissenschaft & Technologie*, vol. 134, p. 110140, 2020.

[26] N. Zhang, C. Huang, and S. Ou, "In vitro binding capacities of three dietary fibers and their mixture for four toxic elements, cholesterol, and bile acid," *Journal of Hazardous Materials*, vol. 186, no. 1, pp. 236–239, 2011.

[27] M. Gu, H. Fang, Y. Gao, T. Su, Y. Niu, and L. Yu, "Characterization of enzymatic modified soluble dietary fiber from tomato peels with high release of lycopene," *Food Hydrocolloids*, vol. 99, Article ID 105321, 2019.

[28] L. Wang, H. Xu, F. Yuan, R. Fan, and Y. Gao, "Preparation and physicochemical properties of soluble dietary fiber from orange peel assisted by steam explosion and dilute acid soaking," *Food Chemistry*, vol. 185, pp. 90–98, 2015.

[29] R.-f. Yang, C. Zhao, X. Chen, S.-w. Chan, and J.-y. Wu, "Chemical properties and bioactivities of Goji (Lycium barbarum) polysaccharides extracted by different methods," *Journal of Functional Foods*, vol. 17, pp. 903–909, 2015.

[30] C.-F. Chau and Y.-L. Huang, "Comparison of the chemical composition and physicochemical properties of different fibers prepared from the peel of citrus sinensis L. Cv. Liucheng," *Journal of Agricultural and Food Chemistry*, vol. 51, no. 9, pp. 2615–2618, 2003.

[31] H. Qiao, H. Shao, X. Zheng et al., "Modification of sweet potato (Ipomoea batatas Lam.) residues soluble dietary fiber following twin-screw extrusion," *Food Chemistry*, vol. 335, Article ID 127522, 2021.

[32] Y. Yi, X.-Y. Huang, Z.-T. Zhong et al., "Structural and biological properties of polysaccharides from lotus root," *International Journal of Biological Macromolecules*, vol. 130, pp. 454–461, 2019.

[33] S. Li, J. Li, Z. Zhu, S. Cheng, J. He, and O. Lamikanra, "Soluble dietary fiber and polyphenol complex in lotus root: preparation, interaction and identification," *Food Chemistry*, vol. 314, p. 126219, 2020.

[34] A. Wen, M. Gui, Y. Peng, H. Wang, X. Jiang, and L. Ren, "Research progress on the effect of fucoidin structure on its function," *Science and Technology of Food Industry*, vol. 40, no. 9, pp. 346–350+356, 2019.

[35] X. Liang, Z. Wang, and J. Li, "Determination of monosaccharide composition of pectin by capillary gas chromatography," *Journal of Northwest Pharmaceutical*, vol. 24, no. 01, pp. 6-7, 2009.

[36] M. Inaba, T. Maruyama, Y. Yoshimi et al., "l-Fucose-containing arabinogalactan-protein in radish leaves," *Carbohydrate Research*, vol. 415, pp. 1–11, 2015.

[37] J. Zhang and Z.-W. Wang, "Soluble dietary fiber from Canna edulis Ker by-product and its physicochemical properties," *Carbohydrate Polymers*, vol. 92, no. 1, pp. 289–296, 2013.

[38] W. Li, S. Cui, and Y. Kakuda, "Extraction, fractionation, structural and physical characterization of wheat β-d-glucans," *Carbohydrate Polymers*, vol. 63, no. 3, pp. 408–416, 2006.

[39] V. Orlien, "Structural changes induced in foods by HPP," *Innovative Food Processing Technologies*, vol. 14, pp. 112–129, 2021.

[40] Y. Chen, R. Ye, L. Yin, and N. Zhang, "Novel blasting extrusion processing improved the physicochemical properties of soluble dietary fiber from soybean residue and in vivo evaluation," *Journal of Food Engineering*, vol. 120, pp. 1–8, 2014.

[41] M. Milas, M. Rinaudo, M. Knipper, and J. L. Schuppiser, "Flow and viscoelastic properties of xanthan gum solutions," *Macromolecules*, vol. 23, no. 9, pp. 2506–2511, 1990.

[42] B.-C. Wu, B. Degner, and D. J. McClements, "Creation of reduced fat foods: influence of calcium-induced droplet aggregation on microstructure and rheology of mixed food dispersions," *Food Chemistry*, vol. 141, no. 4, pp. 3393–3401, 2013.

[43] N. Li, Z. Feng, Y. Niu, and L. Yu, "Structural, rheological and functional properties of modified soluble dietary fiber from tomato peels," *Food Hydrocolloids*, vol. 77, pp. 557–565, 2018.

[44] R. Karimi, M. H. Azizi, and Q. Xu, "Effect of different enzymatic extractions on molecular weight distribution, rheological and microstructural properties of barley bran β-glucan," *International Journal of Biological Macromolecules*, vol. 126, pp. 298–309, 2019.

[45] J. Liu, Z. Wang, Z. Wang et al., "Physicochemical and functional properties of soluble dietary fiber from different colored quinoa varieties (Chenopodium quinoa Willd)," *Journal of Cereal Science*, vol. 95, Article ID 103045, 2020.